

See discussions, stats, and author profiles for this publication at: <https://www.researchgate.net/publication/231626815>

Switching of Pseudorotaxanes and Catenanes Incorporating a Tetrathiafulvalene Unit by Redox and Chemical Input†

ARTICLE *in* THE JOURNAL OF ORGANIC CHEMISTRY · FEBRUARY 2000

Impact Factor: 4.72 · DOI: 10.1021/jo991781t · Source: PubMed

CITATIONS

222

READS

20

9 AUTHORS, INCLUDING:



Alberto Credi

University of Bologna

276 PUBLICATIONS 10,722 CITATIONS

SEE PROFILE

Switching of Pseudorotaxanes and Catenanes Incorporating a Tetrathiafulvalene Unit by Redox and Chemical Inputs[†]

Vincenzo Balzani,^{*,‡} Alberto Credi,[‡] Gunter Matternsteig,[§] Owen A. Matthews,[§] Francisco M. Raymo,^{§,⊥} J. Fraser Stoddart,^{*,§} Margherita Venturi,^{*,‡} Andrew J. P. White,^{||} and David J. Williams^{*,||}

Dipartimento di Chimica "G. Ciamician", Università di Bologna, via Selmi 2, Bologna, I-40126, Italy, Department of Chemistry and Biochemistry, University of California, Los Angeles, 405 Hilgard Avenue, Los Angeles, California 90095-1569, and Department of Chemistry, Imperial College, South Kensington, London, SW7 2AY, UK

Received November 16, 1999

An acyclic polyether **1a**, incorporating a central tetrathiafulvalene (TTF) electron donor unit and two 4-*tert*-butylphenoxy groups at its termini, has been synthesized. Two macrocyclic polyethers containing two different electron donors, namely a TTF unit with, in one case, a 1,4-dioxybenzene ring (**2a**), and, in the other case (**2b**), a 1,5-dioxynaphthalene ring system, have also been synthesized. These two macrocyclic polyethers have been mechanically interlocked in kinetically controlled template-directed syntheses with cyclobis(paraquat-*p*-phenylene) cyclophane (**3⁴⁺**) to afford the [2]catenanes **2a/3⁴⁺** and **2b/3⁴⁺**, respectively. X-ray crystallography reveals that the [2]-catenane **2b/3⁴⁺** has the TTF unit of **2b** located inside the cavity of **3⁴⁺**. The spectroscopic (UV/vis and ¹H NMR) and electrochemical properties of compounds **1a**, **2a**, **2b**, **2a/3⁴⁺**, and **2b/3⁴⁺** and of the [2]pseudorotaxane **1a·3⁴⁺** were investigated. The absorption and emission properties of the mono- and dioxidized forms of the TTF unit in these various species have also been studied. The results obtained in acetonitrile solution can be summarized as follows. (a) While TTF²⁺ exhibits a strong fluorescence, no emission can be observed for the TTF²⁺ units contained in the polyethers and in their pseudorotaxanes and catenanes. (b) A donor–acceptor absorption band is observed upon two-electron oxidation of the TTF unit in the macrocyclic polyethers **2a** and **2b**. (c) The spontaneous self-assembly of **1a** and **3⁴⁺** to give the [2]pseudorotaxane **1a·3⁴⁺** is strongly favored ($K_{\text{ass.}} = 5 \times 10^5 \text{ L mol}^{-1}$) but slow (at 296 K, $k = 11.3 \text{ L mol}^{-1} \text{ s}^{-1}$ and $\Delta G^\ddagger = 15.9 \text{ kcal mol}^{-1}$) because of the steric hindrance associated with the bulky end groups of **1a**. (d) In the pseudorotaxane **1a·3⁴⁺**, the reversible displacement of the cyclophane from the TTF unit in the threadlike substrate occurs on oxidation/reduction of its electroactive components. (e) Switching between the two translational isomers of the catenanes **2a/3⁴⁺** and **2b/3⁴⁺** occurs by cyclic oxidation and reduction of the TTF unit contained in **2a** and in **2b**, respectively. (f) Addition of *o*-chloroanil to the pseudorotaxane **1a·3⁴⁺** and to the catenanes **2a/3⁴⁺** and **2b/3⁴⁺** causes the displacement of the TTF unit from the cavity of the cyclophane **3⁴⁺** because of the formation of an adduct between the TTF unit and *o*-chloroanil.

Introduction

It is well-known¹ that tetrathiafulvalene (TTF) can be oxidized reversibly to TTF⁺ and TTF²⁺. Furthermore, it has been shown² that TTF can behave in charge-transfer complexes as a donor in its neutral form and as an acceptor in its 2+ oxidation state. For these reasons, TTF is an ideal building block with which to construct

supramolecular and molecular systems that can be controlled by external stimuli.^{3,4} In furtherance of our investigations^{2,5,6} on pseudorotaxanes, rotaxanes, and catenanes containing TTF units, we have synthesized three new compounds, namely the acyclic polyether **1a**, bearing a TTF central unit and two 4-*tert*-butylphenoxy terminal groups, the macrocyclic polyethers **2a** and **2b** containing a TTF and either a 1,4-dioxybenzene ring or a 1,5-dioxynaphthalene ring system, respectively. By threading and interlocking these species with the cyclophane cyclobis(paraquat-*p*-phenylene) (**3⁴⁺**), we have generated⁷ (Figure 1) the [2]pseudorotaxane **1a·3⁴⁺** and the [2]catenanes **2a/3⁴⁺** and **2b/3⁴⁺**. In this paper, we describe our investigations of the spectroscopic (UV/vis and ¹H NMR) and electrochemical properties of these systems and compare them with those obtained previously^{5d} for **1b** and **1b·3⁴⁺**. We also discuss the absorption and emission properties of the mono- and di-oxidized forms of the TTF unit in these various complexes and

* Correspondence address: Dr. J. Fraser Stoddart, Department of Chemistry and Biochemistry, University of California, Los Angeles, 405 Hilgard Ave., Los Angeles, CA 90095-1569. Fax: Int. Code. +(310)-206-1843. E-mail: stoddart@chem.ucla.edu.

[†] "Molecular Meccano", Part 54: for Part 53, see: Ashton, P. R.; Balzani, V.; Becher, J.; Credi, A.; Fyfe, M. C. T.; Matternsteig, G.; Menzer, S.; Nielsen, M. B.; Raymo, F. M.; Stoddart, J. F.; Venturi, M.; Williams, D. J. *J. Am. Chem. Soc.* **1999**, *121*, 3951–3957.

[‡] Università di Bologna.

[§] University of California, Los Angeles.

^{||} Imperial College.

[⊥] Current address: Center for Supramolecular Science, Department of Chemistry, University of Miami, 1301 Memorial Drive, Coral Gables, FL 33124-0431.

(1) (a) Hünig, S.; Kiesslich, G.; Quast, H.; Scheutzw, D. *Liebigs Ann. Chem.* **1973**, 310–323. (b) Schukat, G.; Fanghänel, E. *J. Prakt. Chem.* **1985**, *327* (5), 767–774. (c) Jørgensen, T.; Hansen, T. K.; Becher, J. *Chem. Soc. Rev.* **1994**, *23*, 41–51. (d) Nielsen, M. B.; Becher, J. *Liebigs Ann./Recueil* **1997**, 2177–2187.

(2) Ashton, P. R.; Balzani, V.; Becher, J.; Credi, A.; Fyfe, M. C. T.; Matternsteig, G.; Menzer, S.; Nielsen, M. B.; Raymo, F. M.; Stoddart, J. F.; Venturi, M.; Williams, D. J. *J. Am. Chem. Soc.* **1999**, *121*, 3951–3957.

compounds and demonstrate chemical and electrochemical switching between different forms of the pseudorotaxane and catenane species that correspond to changes in the relative positions of their component parts.

(3) For reviews, see: (a) Balzani, V.; Scandola, F. *Supramolecular Photochemistry*; Horwood, Chichester, 1991. (b) Gust, D.; Moore, T. A. *Top. Curr. Chem.* **1991**, *159*, 103–151. (c) Balzani, V. *Tetrahedron* **1992**, *48*, 10443–10514. (d) Bissell, R. A.; de Silva, A. P.; Gunaratne, H. Q. N.; Lynch, P. L. M.; Maguire, G. E. M.; McCoy, C. P.; Sandanayake, K. R. A. S. *Top. Curr. Chem.* **1993**, *168*, 223–264. (e) Swager, T. M.; Marsella, M. J. *Adv. Mater.* **1994**, *6*, 595–597. (f) De Silva, A. P.; McCoy, C. P. *Chem. Ind.* **1994**, 992–996. (g) Fabbri, L.; Poggi, A. *Chem. Soc. Rev.* **1995**, *24*, 197–202. (h) Benniston, A. C. *Chem. Soc. Rev.* **1996**, *25*, 427–435. (i) Shinkai, S. *Comprehensive Supramolecular Chemistry*; Atwood, J. L.; Davies, J. E. D., MacNicol, D. D., Vögtle, F., Eds.; Pergamon: Oxford, 1996; Vol. 1, pp 671–700. (j) de Silva, A. P.; Gunaratne, H. Q. N.; Gunlaugsson, T.; Huxley, A. J. M.; McCoy, C. P.; Rademacher, J. T.; Rice, T. E. *Chem. Rev.* **1997**, *97*, 1515–1566. (k) Ward, M. D. *Chem. Ind.* **1997**, 640–645. (l) *Modular Chemistry*; Michl, J., Ed.; Kluwer Academic Publishers: Dordrecht, 1997. (m) Beer, P. D. *Acc. Chem. Res.* **1998**, *31*, 71–80. (n) Swager, T. M. *Acc. Chem. Res.* **1998**, *31*, 201–207. (o) Boulas, P. L.; Gómez-Kaifer, M.; Echegoyen, L. *Angew. Chem., Int. Ed.* **1998**, *37*, 216–247. (p) Balzani, V.; Gómez-López, M.; Stoddart, J. F. *Acc. Chem. Res.* **1998**, *31*, 405–414. (q) Sauvage, J.-P. *Acc. Chem. Res.* **1998**, *31*, 611–619. (r) Niemz, A.; Rotello, V. M. *Acc. Chem. Res.* **1999**, *32*, 42–52. (s) Kaifer, A. E. *Acc. Chem. Res.* **1999**, *32*, 62–71. (t) Piotrowski, P. *Chem. Soc. Rev.* **1999**, *28*, 143–150.

(4) For recent papers, see: (a) Willner, I.; Willner, B. *Adv. Mater.* **1997**, *9*, 351–355. (b) Ashton, P. R.; Ballardini, R.; Balzani, V.; Boyd, S. E.; Credi, A.; Gandolfi, M. T.; Gómez-López, M.; Iqbal, S.; Philp, D.; Prece, J. A.; Prodi, L.; Ricketts, H. G.; Stoddart, J. F.; Tolley, M. S.; Venturi, M.; White, A. J. P.; Williams, D. J. *Chem. Eur. J.* **1997**, *3*, 152–170. (c) Deans, R.; Niemz, A.; Breinlinger, E. C.; Rotello, V. M. *J. Am. Chem. Soc.* **1997**, *119*, 10863–10864. (d) Livoreil, A.; Sauvage, J.-P.; Armaroli, N.; Balzani, V.; Flamigni, L.; Ventura, B. *J. Am. Chem. Soc.* **1997**, *119*, 12114–12124. (e) Wang, Y.; Alvarez, J.; Kaifer, A. E. *Chem. Commun.* **1998**, 1457–1458. (f) Takashita, M.; Irie, M. *J. Org. Chem.* **1998**, *63*, 6643–6649. (g) Archut, A.; Azzellini, G. C.; Balzani, V.; De Cola, L.; Vögtle, F. *J. Am. Chem. Soc.* **1998**, *120*, 12187–12191. (h) Steinberg-Yfrach, G.; Rigaud, J.-L.; Durantini, E. N.; Moore, A. L.; Gust, D.; Moore, T. A. *Nature* **1998**, *392*, 479–482. (i) de Silva, A. P.; Dixon, I. M.; Gunaratne, H. Q. N.; Gunlaugsson, T.; Maxwell, P. R. S.; Rice, T. E. *J. Am. Chem. Soc.* **1999**, *121*, 1393–1394. (j) Fabbri, L.; Gatti, F.; Pallavicini, P.; Zambbarbieri, E. *Chem. Eur. J.* **1999**, *5*, 682–690. (k) Asakawa, M.; Ashton, P. R.; Balzani, V.; Brown, C. L.; Credi, A.; Menzer, S.; Newton, S. P.; Raymo, F. M.; Shipway, A. N.; Spencer, N.; Quick, A.; Stoddart, J. F.; White, A. J. P.; Williams, D. J. *Chem. Eur. J.* **1999**, *5*, 860–875. (l) Ishow, E.; Credi, A.; Balzani, V.; Spadola, F.; Mandolini, L. *Chem. Eur. J.* **1999**, *5*, 984–989.

(5) (a) Philp, D.; Slawin, A. M. Z.; Spencer, N.; Stoddart, J. F.; Williams, D. J. *J. Chem. Soc., Chem Commun.* **1991**, 1584–1586. (b) Ashton, P. R.; Bissell, R. A.; Górski, R.; Philp, D.; Spencer, N.; Stoddart, J. F.; Tolley, M. S. *Synlett* **1992**, 919–922. (c) Anelli, P.-L.; Asakawa, M.; Ashton, P. R.; Bissell, R. A.; Clavier, G.; Górski, R.; Kaifer, A. E.; Langford, S. J.; Mattersteig, G.; Menzer, S.; Philp, D.; Slawin, A. M. Z.; Spencer, N.; Stoddart, J. F.; Tolley, M. S.; Williams, D. J. *Chem. Eur. J.* **1997**, *3*, 1113–1135. (d) Asakawa, M.; Ashton, P. R.; Balzani, V.; Credi, A.; Mattersteig, G.; Matthews, O. A.; Montalti, M.; Spencer, N.; Stoddart, J. F.; Venturi, M. *Chem. Eur. J.* **1997**, *3*, 1992–1996. (e) Asakawa, M.; Ashton, P. R.; Balzani, V.; Credi, A.; Hamers, C.; Mattersteig, G.; Montalti, M.; Shipway, A. N.; Spencer, N.; Stoddart, J. F.; Tolley, M. S.; Venturi, M.; White, A. J. P.; Williams, D. J. *Angew. Chem., Int. Ed.* **1998**, *37*, 333–337. (f) Credi, A.; Balzani, V.; Langford, S. J.; Montalti, M.; Raymo, F. M.; Stoddart, J. F. *New J. Chem.* **1998**, *22*, 1061–1065. (g) Asakawa, M.; Ashton, P. R.; Balzani, V.; Boyd, S. E.; Credi, A.; Mattersteig, G.; Menzer, S.; Montalti, M.; Raymo, F. M.; Ruffilli, C.; Stoddart, J. F.; Venturi, M.; Williams, D. J. *Eur. J. Org. Chem.* **1999**, 985–994.

(6) For related pseudorotaxanes, rotaxanes, and catenanes containing TTF units, see: (a) Jørgensen, T.; Becher, J.; Chambron, J.-C.; Sauvage, J.-P. *Tetrahedron Lett.* **1994**, *35*, 4339–4342. (b) Li, Z. T.; Stein, P. C.; Svenstrup, N.; Lund, K. H.; Becher, J. *Angew. Chem., Int. Ed. Engl.* **1995**, *34*, 2524–2528. (c) Li, Z. T.; Becher, J. *Chem. Commun.* **1996**, 639–640. (d) Li, Z. T.; Stein, P. C.; Becher, J.; Jensen, D.; Mørk, P.; Svenstrup, N. *Chem. Eur. J.* **1996**, *2*, 624–633. (e) Devonport, M.; Blower, M. A.; Bryce, M. R.; Goldenberg, L. M. *J. Org. Chem.* **1997**, *62*, 885–887. (f) Becher, J.; Li, Z. T.; Blanchard, P.; Svenstrup, N.; Lau, J.; Nielsen, M. B.; Leriche, P. *Pure Appl. Chem.* **1997**, *69*, 465–470. (g) Li, Z. T.; Becher, J. *Synlett* **1997**, 557–560. (h) Nielsen, M. B.; Thorup, N.; Becher, J. *J. Chem. Soc., Perkin Trans. 1* **1998**, 1305–1308.

(7) The [2]pseudorotaxanes and the [2]catenanes are labeled with the numbers of their two components separated by the symbols “·” and “/”, respectively.

Results and Discussion

Synthesis. The macrocyclic polyethers **2a** and **2b** were obtained^{5c} (Scheme 1) as mixtures of their *cis*- and *trans*-isomers by reacting a mixture⁸ of the *cis*- and *trans*-isomers of **4** with **5a** and **5b**, respectively, under high dilution conditions. Reaction of **6**[PF₆]₂ with **7**, in the presence of either **2a** or **2b**, afforded^{5c} the corresponding [2]catenanes **2a/3**[PF₆]₄ or **2b/3**[PF₆]₄, after counterion exchange. The acyclic polyether **1a** was obtained (Scheme 2) as a mixture of its *cis*- and *trans*-isomers by reacting a mixture⁸ of the *cis*- and *trans*-isomers of **4** with **8**, following a procedure already used for the synthesis of **1b**.^{5d}

X-ray Crystallography. Only the *trans*-isomer of the [2]catenane **2b/3**[PF₆]₄ is observed^{5c} (Figure 2a) in the solid state. The TTF unit is inserted through the cavity of the tetracationic cyclophane, while the 1,5-dioxynaphthalene ring system resides alongside. The central [C=C] bond of the TTF unit and the [O··O] axis of the 1,5-dioxynaphthalene ring system subtend angles of 74° and 18°, respectively, to the mean plane of the tetracationic cyclophane (defined by the four methylene carbon atoms). The mean interplanar separations between the TTF unit and the “inside” and “alongside” bipyridinium units and between the 1,5-dioxynaphthalene ring system and the “inside” bipyridinium unit are 3.43, 3.37, and 3.31 Å, respectively. Two of the diametrically opposite α-bipyridinium hydrogen atoms on the “inside” bipyridinium unit sustain [C–H··O] hydrogen bonds with, in one instance, the first and, in the other, the second polyether oxygen atoms (counting from the TTF unit); the [C··O] distances are 3.39 and 3.12 Å and the corresponding [H··O] distances and [C–H··O] angles are 2.43, 2.40 Å and 174° 132°, respectively. The [2]catenane molecules pack to form π-donor/π-acceptor stacks (Figure 2b) with an interplanar separation of 3.29 Å between the “alongside” 1,5-dioxynaphthalene ring system of one molecule and the “alongside” bipyridinium unit of another.

Spectroscopic Properties. Components. The acyclic and macrocyclic polyethers **1a** and **1b**,^{5d} and **2a** and **2b**, respectively, show the absorption bands of their chromophoric units which are TTF, for all the compounds, and phenoxy, 1,4-dioxybenzene,⁹ and 1,5-dioxynaphthalene¹⁰ for **1a**, **2a**, and **2b**, respectively. The fluorescence of the phenoxy,⁹ 1,4-dioxybenzene,⁹ and 1,5-dioxynaphthalene¹⁰ units cannot be observed, presumably because it is quenched via energy or electron transfer by the nonemitting² TTF unit. Upon addition of Fe(ClO₄)₃, spectral changes are observed as expected^{5f} for the successive one-electron oxidation of the TTF unit to TTF⁺ and TTF²⁺. In the case of crown **2b** (Figure 3), it is also

(8) Compound **4** was obtained as a mixture of *cis*- and *trans*-isomers. This mixture was employed as the starting material in the numerous syntheses. Compounds **1a**, **2a**, **2b**, **2a/3**[PF₆]₄, and **2b/3**[PF₆]₄ were also obtained as mixtures of their *cis*- and *trans*-isomers. All attempts to separate the two isomers of these compounds were unsuccessful. For the synthesis of **4**, see: Andreu, R.; Garin, J.; Orduna, J.; Saviron, M.; Cousseau, J.; Gorgues, A.; Morrisson, V.; Nozdryn, T.; Becher, J.; Clausen, R. P.; Bryce, M. R.; Skabara, P. J.; Dehaen, W. *Tetrahedron Lett.* **1994**, *35*, 9243–9246.

(9) Amabilino, D. B.; Asakawa, M.; Ashton, P. R.; Ballardini, R.; Balzani, V.; Belohradsky, M.; Credi, A.; Higuchi, M.; Raymo, F. M.; Shimizu, T.; Stoddart, J. F.; Venturi, M.; Yase, K. *New J. Chem.* **1998**, *22*, 959–972.

(10) Ashton, P. R.; Ballardini, R.; Balzani, V.; Credi, A.; Gandolfi, M. T.; Menzer, S.; Pérez-García, L.; Prodi, L.; Stoddart, J. F.; Venturi, M.; White, A. J. P.; Williams, D. J. *J. Am. Chem. Soc.* **1995**, *117*, 11171–11197.

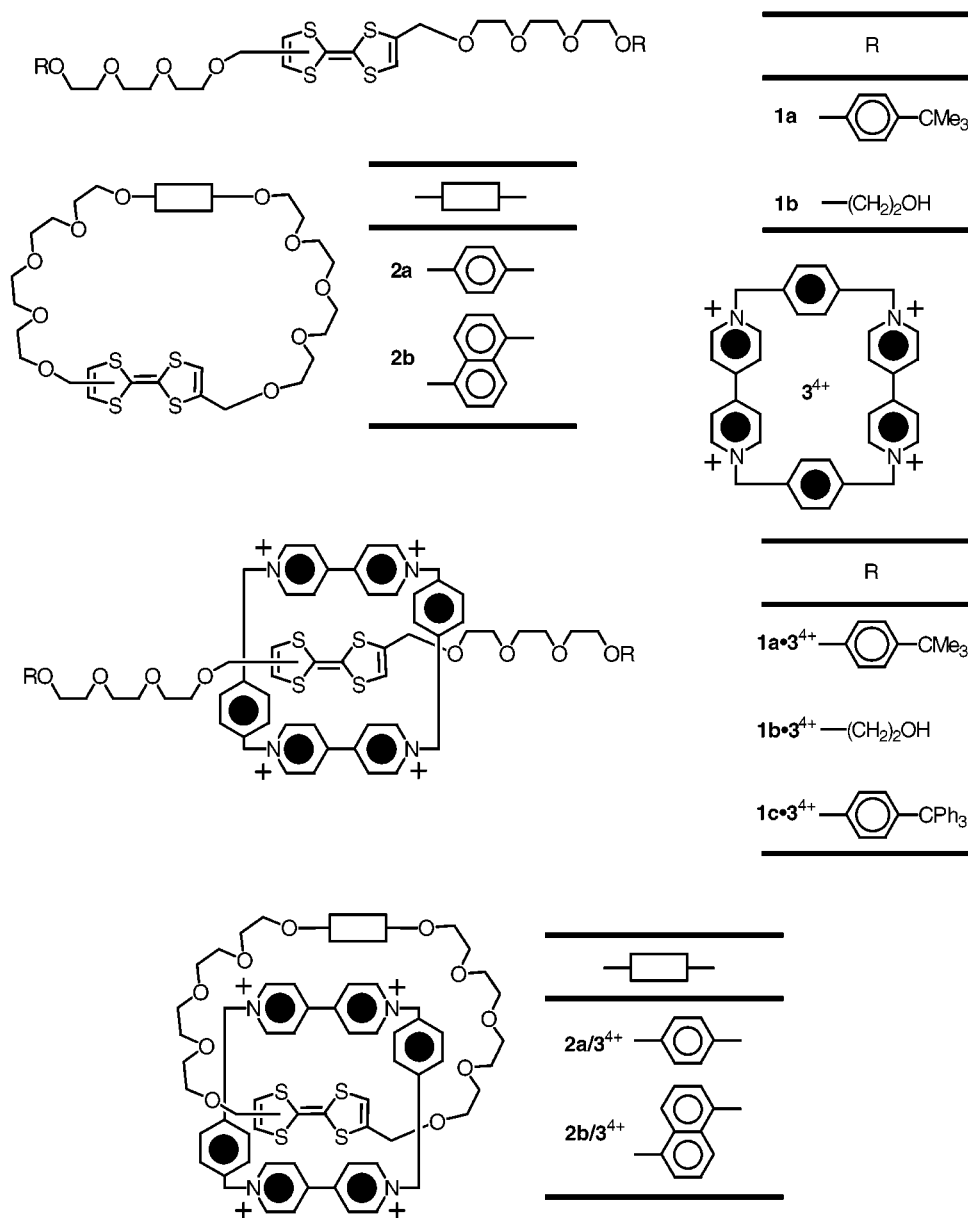


Figure 1. Structural formulas of the examined compounds.

possible to observe the presence of a broad band at low energy ($\lambda_{\text{max}} = 805 \text{ nm}$) which can be assigned to the intramolecular charge-transfer (CT) interaction of the 1,5-dioxynaphthalene donor unit with the TTF^{2+} acceptor unit.² In the case of crown **2a**, the CT band is displaced, as expected, toward higher energy because of the higher oxidation potential of 1,4-dioxybenzene compared with that of 1,5-dioxynaphthalene,¹¹ and partially overlaps with the tail of the more intense TTF^{2+} band with a maximum at 390 nm. No evidence of a CT band is present in the acyclic polyethers. It is worth noting that while TTF^{2+} exhibits a strong fluorescence, no emission can be observed for the TTF^{2+} units contained in the polyethers. This observation is not surprising since the fluorescent excited state of TTF^{2+} is a strong oxidant (reduction potential about +3.6 V vs SCE)² and can therefore be quenched, as we have verified¹² in independent experiments, even by aliphatic ethers.

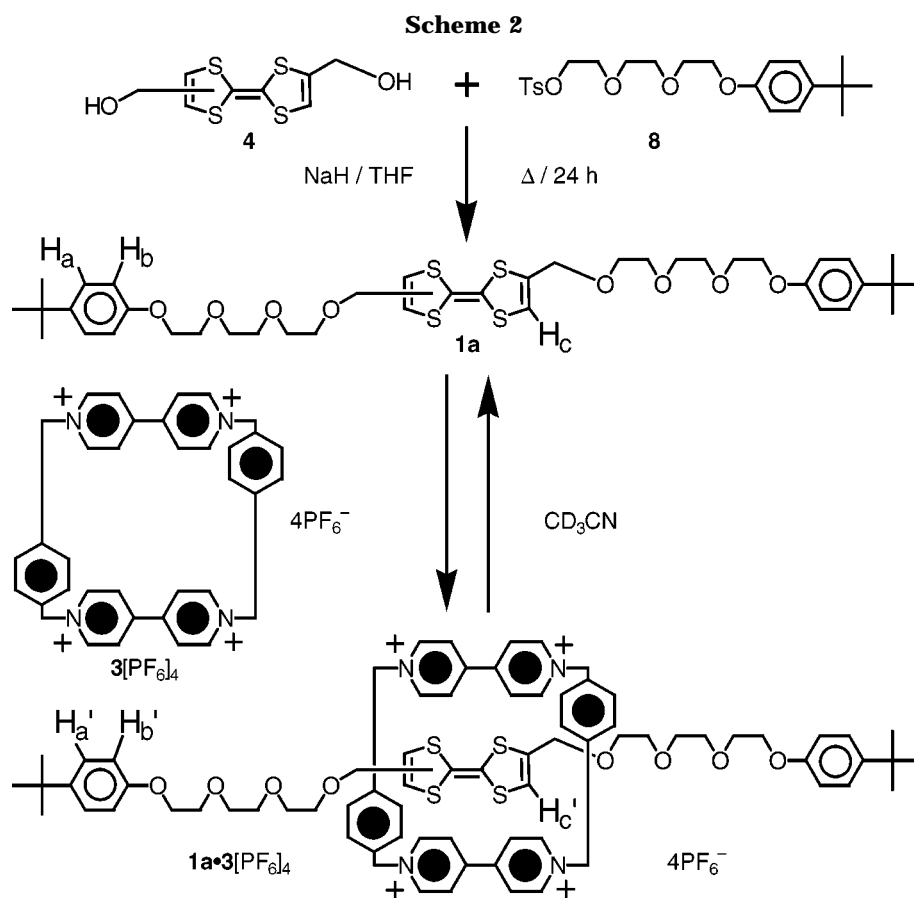
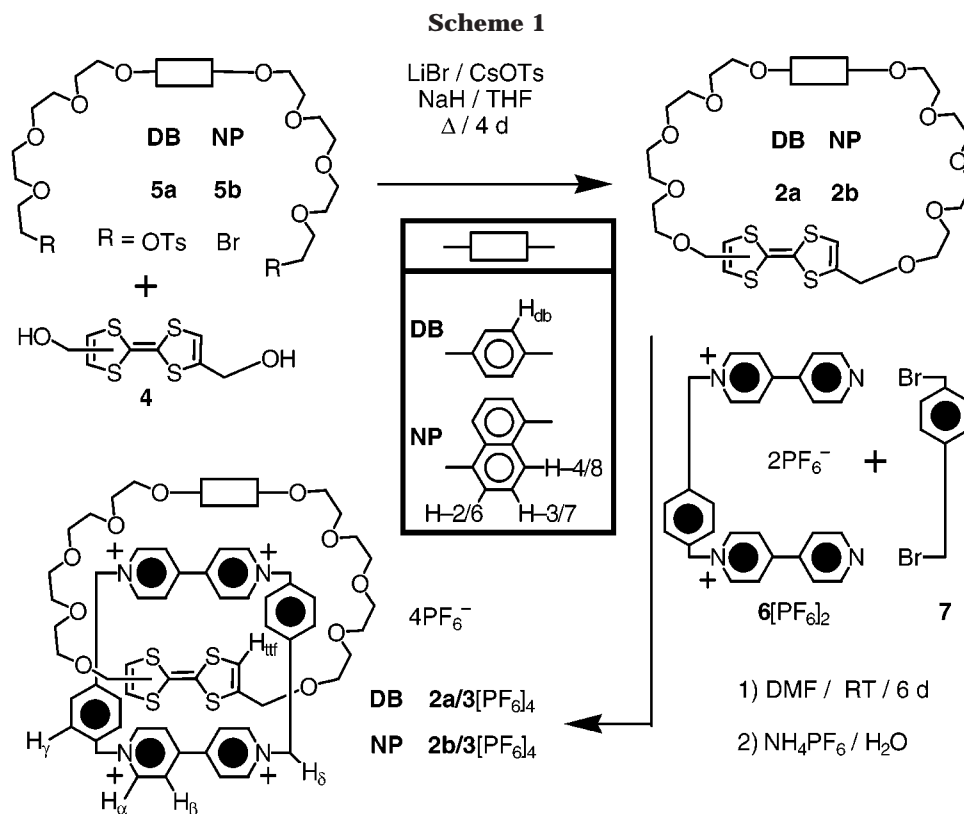
Catenanes **2a/3⁴⁺ and **2b/3⁴⁺**.** Since TTF is a better electron donor than 1,4-dioxybenzene and 1,5-dioxynaphthalene, it is to be expected that the most stable trans-

lational isomer for catenanes **2a/3⁴⁺** and **2b/3⁴⁺** is that in which the TTF unit occupies the cavity of the electron-accepting tetracationic cyclophane. This expectation was confirmed (vide supra) by the X-ray crystal structure^{5e} of **2b/3**[PF₆]₄, as well as by the ¹H NMR spectra of both compounds. The absorption spectra are also consistent with such a coconformation.¹³ For both catenanes (see Figure 4 for the spectrum of **2a/3⁴⁺**), a broad and relatively weak band is found at low energy ($\lambda_{\text{max}} = 835 \text{ nm}$), besides the strong bands below 400 nm related to the TTF, 1,4-dioxybenzene or 1,5-dioxynaphthalene, and 4,4'-bipyridinium chromophoric groups. Such a low energy band is expected for the CT interaction that origi-

(11) Asakawa, M.; Ashton, P. R.; Ballardini, R.; Balzani, V.; Belohradsky, M.; Gandolfi, M. T.; Kocian, O.; Prodi, L.; Raymo, F. M.; Stoddart, J. F.; Venturi, M. *J. Am. Chem. Soc.* **1997**, *119*, 302–310.

(12) The presence of $8 \times 10^{-3} \text{ mol L}^{-1}$ dicyclohexano-24-crown-8 causes 50% quenching in the emission of a $1 \times 10^{-4} \text{ mol L}^{-1}$ TTF^{2+} in MeCN solution ($\lambda_{\text{ex}} = 350 \text{ nm}$).

(13) For a definition of the term “coconformation”, see: Fyfe, M. C. T.; Glink, P. T.; Menzer, S.; Stoddart, J. F.; White, A. J. P.; Williams, D. J. *Angew. Chem., Int. Ed. Engl.* **1997**, *36*, 2068–2070.



nates when the electron donor TTF unit is located inside the electron-accepting tetracationic cyclophane.^{5d,e} For **2a/3**⁴⁺, no CT band around 470 nm, which would result from the 1,4-dioxybenzene ring being located inside the cyclophane,¹⁴ can be detected; analogously, the CT band char-

acteristic of the encirclement of the 1,5-dioxynaphthalene unit by **3**⁴⁺ ($\lambda_{\text{max}} = 515 \text{ nm}$)^{4b,10} does not appear in the spectrum of **2b/3**⁴⁺. Upon oxidation of **2a/3**⁴⁺ and **2b/3**⁴⁺ with Fe(ClO₄)₃, the CT band with $\lambda_{\text{max}} = 835 \text{ nm}$ disappears and the absorption features of the TTF⁺ and TTF²⁺

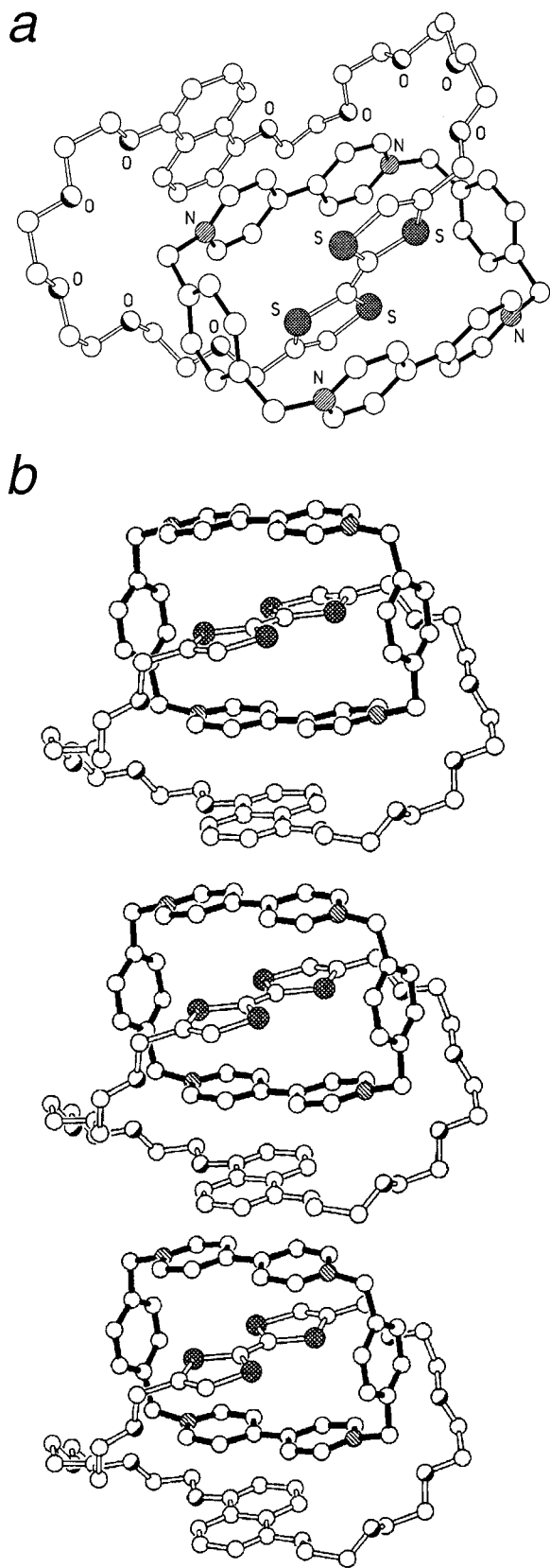


Figure 2. (a) Ball-and-stick representation of the solid-state structure of the [2]catenane **2b/3⁴⁺**. (b) Part of one of the continuous polar stacks present in the crystals of **2b/3⁴⁺**.

units reveal themselves in the visible region. At the end of the two-electron oxidation of **2b/3⁴⁺**—achieved after addition of 2 equiv of $\text{Fe}(\text{ClO}_4)_3$ —the band characteristic of the inclusion of the 1,5-dioxynaphthalene moiety into

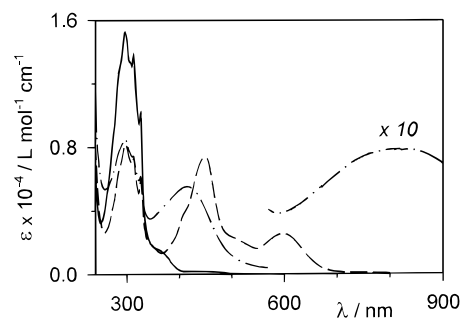


Figure 3. Absorption spectrum (MeCN solution, room temperature) of the macrocyclic polyether **2b** (—), and of the same solution after addition of 1 (— —) and 2 (· · ·) equiv of $\text{Fe}(\text{ClO}_4)_3$.

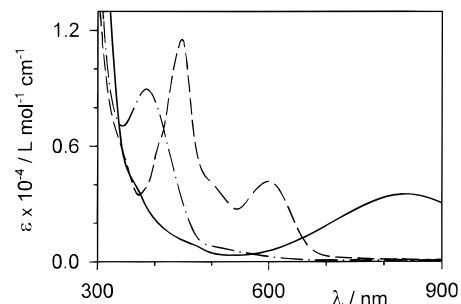


Figure 4. Absorption spectrum (MeCN solution, room temperature) of the [2]catenane **2a/3⁴⁺** (—), and of the same solution after addition of 1 (— —) and 2 (· · ·) equiv of $\text{Fe}(\text{ClO}_4)_3$.

the cyclophane^{4b,10} can be seen. Under the same conditions, it is possible to observe for **2a/3⁴⁺** a broad band with a maximum around 500 nm (Figure 4), partially covered by the tail of the more intense TTF^{2+} band, that can be assigned to the presence of the 1,4-dioxybenzene ring inside the cyclophane.¹⁴ Since the electrochemical results show that the TTF unit is expelled from the cavity of **3⁴⁺** after its first oxidation, the CT band characteristic of the inclusion of the 1,4-dioxybenzene or 1,5-dioxynaphthalene units into **3⁴⁺** should be present already after addition of 1 equiv of $\text{Fe}(\text{ClO}_4)_3$. At this stage, however, such a band cannot be detected since it falls in a spectral region dominated by the strong absorption of the TTF^+ monocation (Figure 4). Regardless of the oxidation state, as expected, no emission is observed from the TTF or from the 1,4-dioxybenzene or 1,5-dioxynaphthalene moieties because of the presence of low energy CT excited states.^{10,14}

Pseudorotaxane 1a·3⁴⁺. Pseudorotaxanes are obtained under thermodynamic control upon mixing their acyclic and cyclic components in solution, and the occurrence of the threading process can be evidenced by their ¹H NMR, absorption, and emission spectra.^{4b,5d,f,14} The threading rate is related to the structures of the molecular components of the pseudorotaxane, and in particular by the sizes of the end groups of the thread compared to the dimension of the ring's cavity.^{15,16} Slipping of macrocycles over the bulky end groups of the dumbbell-shaped component has already been used to self-assemble

(14) Anelli, P.-L.; Ashton, P. R.; Ballardini, R.; Balzani, V.; Delgado, M.; Gandolfi, M. T.; Goodnow, T. T.; Kaifer, A. E.; Philp, D.; Pietraszkiewicz, M.; Prodi, L.; Reddington, M. V.; Slawin, A. M. Z.; Spencer, N.; Stoddart, J. F.; Vicent, C.; Williams, D. J. *J. Am. Chem. Soc.* **1992**, *114*, 193–218.

(15) Ashton, P. R.; Baxter, I.; Fyfe, M. C. T.; Raymo, F. M.; Spencer, N.; Stoddart, J. F.; White, A. J. P.; Williams, D. J. *J. Am. Chem. Soc.* **1998**, *120*, 2297–2307.

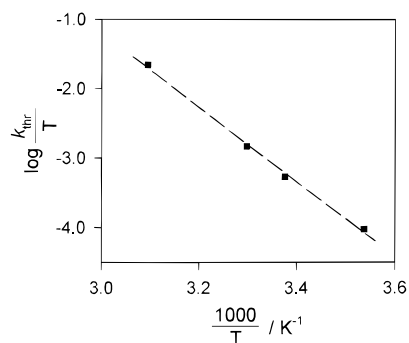


Figure 5. Temperature dependence (Eyring plot) of the rate constant for the threading process (k_{thr}) between **1a** and **3⁴⁺** (MeCN solution) in the temperature range 9.5–50 °C.

rotaxanes.^{11,16} In this regard, it has been concluded¹⁵ that a definite cutoff between rotaxanes and pseudorotaxanes does not exist.

We have previously reported^{5d} that, on mixing equimolar amounts (5×10^{-4} mol L⁻¹) of **1b** and **3⁴⁺**, the [2]-pseudorotaxane **1b·3⁴⁺** is immediately formed as shown by the color change related to the CT interaction ($\lambda_{\text{max}} = 830$ nm). We have found, however, that in the case of **1a**, the color ($\lambda_{\text{max}} = 850$ nm) develops much more slowly. The rate constant for the threading process is 11.3 L mol⁻¹ s⁻¹ at 296 K. The stoichiometry (1:1), association constant (5×10^5 L mol⁻¹), and molar absorption coefficient (3300 L mol⁻¹ cm⁻¹ at 850 nm) were obtained from titrations. Experiments, carried out in the temperature range 9.5–50 °C (Figure 5), yielded the following activation parameters: $\Delta H^\ddagger = 10.7$ kcal mol⁻¹; $\Delta S^\ddagger = -17.7$ cal mol⁻¹ K⁻¹. Clearly, the 4-*tert*-butylphenoxy terminal groups of **1a** impose some steric hindrance upon the threading process. At room temperature, the **1a·3⁴⁺** species has some rotaxane as well as some pseudorotaxane character.¹⁵

It should be noted that **1a** contains three electron-donor units, namely a TTF unit in the center and two phenoxy groups bearing *tert*-butyl substituents at its ends. The TTF unit is a much better electron donor than the phenoxy units. Therefore, in **1a·3⁴⁺**, as observed in **1b·3⁴⁺**, the cyclophane **3⁴⁺** is located around the TTF unit, as shown by the presence of a CT band at $\lambda_{\text{max}} = 850$ nm. From the association constants of the cyclophane **3⁴⁺** with **1a** or **1b** (5×10^5 L mol⁻¹)^{5d,17} and an analogous dumbbell-shaped compound containing a 1,4-dioxybenzene ring (2×10^3 L mol⁻¹)¹⁴ in place of the TTF unit, we can estimate that the difference in the stabilization energy between the two types of “stations” for **3⁴⁺** ‘shuttling’ back and forth along **1a** has to be larger than 3.2 kcal mol⁻¹.¹⁸ The energy profile associated with **1a·3⁴⁺** as a function of the ring’s position is illustrated in Figure 6.

Upon addition of 1 equiv of Fe(ClO₄)₃ to a **1a·3⁴⁺** solution, the green color disappears immediately and the absorption features of the TTF⁺ radical cation can be

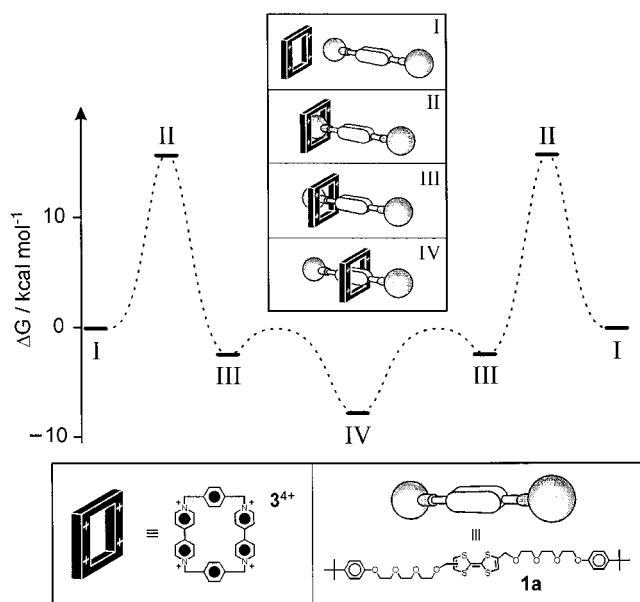


Figure 6. Schematic illustration of the free energy change (MeCN, 296 K) upon varying the relative position of the two components of the [2]pseudorotaxane **1a·3⁴⁺**. The dotted curve has no quantitative meaning. Upon oxidation of the TTF unit of the acyclic component **1a**, the free energy of the co-conformation IV is expected to increase strongly because the stabilizing charge-transfer interaction is destroyed and electrostatic repulsion arises between the TTF⁺ cation and the tetracationic cyclophane.

observed. To understand whether the one-electron oxidation of the TTF unit causes dethreading, the experiment has been carried out in the presence of an acyclic polyether containing a 1,5-dioxynaphthalene unit, namely 1,5-bis[2-[2-(2-hydroxyethoxy)ethoxy]ethoxy]naphthalene, whose fluorescence is quenched upon insertion^{5f,19} into the cavity of the cyclophane **3⁴⁺**. Indeed, such a fluorescence quenching is observed but does not follow immediately upon addition of Fe(ClO₄)₃, thus allowing us to study the dethreading kinetics of **3⁴⁺** from the radical cation of **1a**. Despite the large errors involved in these measurements,²⁰ the fluorescence decrease can be reasonably fitted with a first-order kinetic equation, giving a value for the dethreading rate constant of (0.2 ± 0.1) s⁻¹ at 296 K.

Electrochemical Behavior. Components. The electrochemical properties of **1a**, **2a**, **2b**, and **3⁴⁺** are summarized in Table 1, where the data for **1b**^{5d} are also reported for comparison purposes. The TTF unit shows its two typical reversible and monoelectronic oxidation processes in both the acyclic **1a** (curve f, Figure 7) and

(18) Since the phenoxy ring is much poorer electron donor than the 1,4-dioxybenzene one, as indicated by the potential values at which these units are oxidized (see ref 9), it is expected to give a weaker interaction with **3⁴⁺**.

(19) Since the association constant between **3⁴⁺** and 1,5-bis[2-[2-(2-hydroxyethoxy)ethoxy]ethoxy]naphthalene is much smaller than that between **3⁴⁺** and **1a**, addition of 4×10^{-5} mol L⁻¹ of the 1,5-dioxynaphthalene-based thread to a MeCN solution containing 4×10^{-5} mol L⁻¹ **3⁴⁺** and 4×10^{-5} mol L⁻¹ **1a** does not substantially perturb the formation of pseudorotaxane **1a·3⁴⁺**. Stopped-flow absorption experiments have shown that the threading of the 1,5-dioxynaphthalene-based thread through the cavity of **3⁴⁺** is very fast and can be considered instantaneous on the time scale of the present experiment (Hammarström, L.; Balzani, V.; Stoddart, J. F. Work in progress).

(20) Credi, A.; Prodi, L. *Spectrochim. Acta A* **1998**, *54*, 159–170.

(16) (a) Ashton, P. R.; Ballardini, R.; Balzani, V.; Belohradsky, M.; Gandolfi, M. T.; Philp, D.; Prodi, L.; Raymo, F. M.; Reddington, M. V.; Spencer, N.; Stoddart, J. F.; Venturi, M.; Williams, D. J. *J. Am. Chem. Soc.*, **1996**, *118*, 4931–4951. (b) Raymo, F. M.; Houk, K. N.; Stoddart, J. F. *J. Am. Chem. Soc.* **1998**, *120*, 9318–9322.

(17) On account of a typographical error, the value (5×10^4 L mol⁻¹) of the association constant reported in ref 5d for the complex **1b·3⁴⁺** is smaller by 1 order of magnitude than the correct value which is, in fact, 5×10^5 L mol⁻¹.

Table 1. Electrochemical Data^a for the Molecular Components.

compound	oxidation ^b	reduction ^b
1a	+0.35; +0.71; +1.57 ^c	—
1b	+0.35; +0.70	—
2a	+0.32; +0.71; +1.34 ^c	—
2b	+0.28; +0.70; +1.17; ^c +1.29 ^c	—
3⁴⁺	—	-0.28; ^d -0.72 ^d

^a Argon-purged MeCN, room temperature, Et₄NPF₆ as supporting electrolyte, glassy carbon as working electrode. ^b Halfwave potential values in V vs SCE; reversible and monoelectronic processes, unless otherwise indicated. ^c Not fully reversible process; potential value estimated from DPV peaks. ^d Two-electron reversible process.

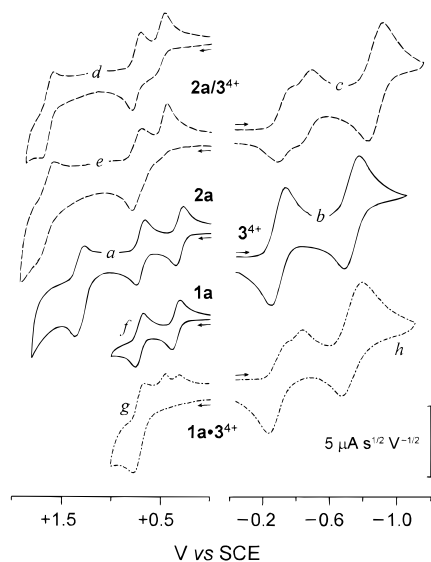


Figure 7. Normalized cyclic voltammetric patterns of the components **1a**, **2a**, and **3⁴⁺** (—), of the [2]catenane **2a/3⁴⁺** (—), and of the [2]pseudorotaxane **1a·3⁴⁺** (---). Argon purged MeCN solution, 5×10^{-4} mol L⁻¹ sample, 0.05 mol L⁻¹ Et₄NPF₆, room temperature, glassy carbon working electrode (0.08 cm²). Ordinate scale: $i/i_{1/2}$ vs potential, where i = current intensity; v = scan rate; differences in the diffusion coefficient of the various species have been taken into account. Curves a, b, and c: 50 mV s⁻¹; curve d: 20 mV s⁻¹; curve e: 500 mV s⁻¹; curves f, g, and h: 200 mV s⁻¹.

cyclic **2a** (curve a, Figure 7) and **2b** polyethers. The other oxidation processes are associated with the *tert*-butylphenoxy groups of the stoppers in **1a** and with the 1,4-dioxybenzene and 1,5-dioxynaphthalene ring systems in **2a** and **2b**, respectively. As far as crown ether **2a** is concerned, the first oxidation of the TTF unit takes place at a potential which is slightly (30 mV) less positive than that of the TTF unit in either **1a** or **1b**. This observation can be accounted for by the presence of stacking interactions between the two π -electron donor units of **2a**, as previously observed for similar crown ethers.^{2,21} The potential at which the oxidation of the 1,4-dioxybenzene ring occurs in **2a** is displaced 70 mV toward more positive values compared with that of the model compound, 1,4-dimethoxybenzene.²¹ This result is consistent with a CT interaction between such π -electron rich systems and the bis-oxidized TTF moiety as evidenced (vide supra) by

absorption spectroscopy. However, a corresponding cathodic shift of the reduction potential value of the TTF²⁺ unit, compared to **1a**, is not observed. This is consistent with the observation that the reduction potential of TTF²⁺ is only very slightly affected, even when TTF²⁺ is sandwiched between two strong electron-donating 1,5-dioxynaphthalene ring systems.² The behavior of **2b**^{5e} is similar to that of **2a**. The larger shift toward less positive potential values (70 mV) of the oxidation of the TTF unit with respect to **1a** can be explained on the basis of the more-extended π -system of the 1,5-dioxynaphthalene unit compared to that of the 1,4-dioxybenzene ring. As observed for **2a**, the second oxidation of the TTF unit of **2b** occurs at the same potential as that of **1a**. On going to more positive potentials, two not fully reversible processes are encountered (Table 1), both of which can be assigned to the oxidation of the 1,5-dioxynaphthalene ring system and both of which are displaced toward more positive potential values compared with the model compound, 1,5-dimethoxynaphthalene ($E_{ox} = +1.11$ V). The differential pulse voltammetric peak corresponding to the first process has an area approximately seven times smaller than that of the second process.²² This behavior can once again be explained by considering that a CT interaction exists between the TTF²⁺ unit and the 1,5-dioxynaphthalene ring system, as evidenced by absorption spectroscopy (vide supra); the presence of two distinct oxidation processes involving the 1,5-dioxynaphthalene unit may be attributed to the different behavior of the *cis*- and *trans*-isomers of **2b**. The tetracationic cyclophane **3⁴⁺** shows (curve b in Figure 7) the two well-known reversible two-electron processes assigned to the simultaneous first and second reductions of the two bipyridinium units.^{11,14}

Catenanes 2a/3⁴⁺ and 2b/3⁴⁺. Upon oxidation of the catenanes **2a/3⁴⁺** and **2b/3⁴⁺**, the electroactive components are the cyclic polyethers **2a** and **2b**, respectively. Since the ¹H NMR spectroscopic data show that the only observed isomer of this catenane has the TTF unit residing in the "inside" position, the first oxidation of the TTF unit should be displaced toward more positive potentials relative to those of **2a**. This prediction is confirmed by the experimental results. However, contrary to what happens in **2a**, the first oxidation process of the TTF unit is characterized by a very large separation between the anodic and the cathodic cyclic voltammetric peaks (Figure 7, curves d and e). On increasing the scan rate, the former moves toward more positive potentials and the latter toward less positive potentials. At a scan rate of 500 mV s⁻¹, there is only one anodic peak at +0.79 V vs SCE (Figure 7, curve e) whose current intensity indicates the occurrence of a bielectronic process. Therefore, at this potential, the second oxidation of TTF also takes place; this process is reversible (half-wave potential +0.76 V vs SCE) as indicated by the cathodic part of the scan. The oxidation of the 1,4-dioxybenzene ring is strongly displaced toward positive potentials (+1.65 V vs SCE; Figure 7, curves d and e) relative to those of **2a** (Figure 7, curve a). The scan-rate dependence of the separation between the anodic and cathodic peaks of the first oxidation process of the TTF unit of **2a/3⁴⁺** indicates

(21) Ballardini, R.; Balzani, V.; Credi, A.; Brown, C. L.; Gillard, R. E.; Montalti, M.; Philp, D.; Stoddart, J. F.; Venturi, M.; White, A. J. P.; Williams, B. J.; Williams, D. J. *J. Am. Chem. Soc.* **1997**, *119*, 12503–12513.

(22) None of these process can be attributed to 1,5-dioxynaphthalene-type impurities since (i) the potential values are different from that of the model compound, and (ii) the presence of such impurities would have been clearly evidenced by luminescence measurements.

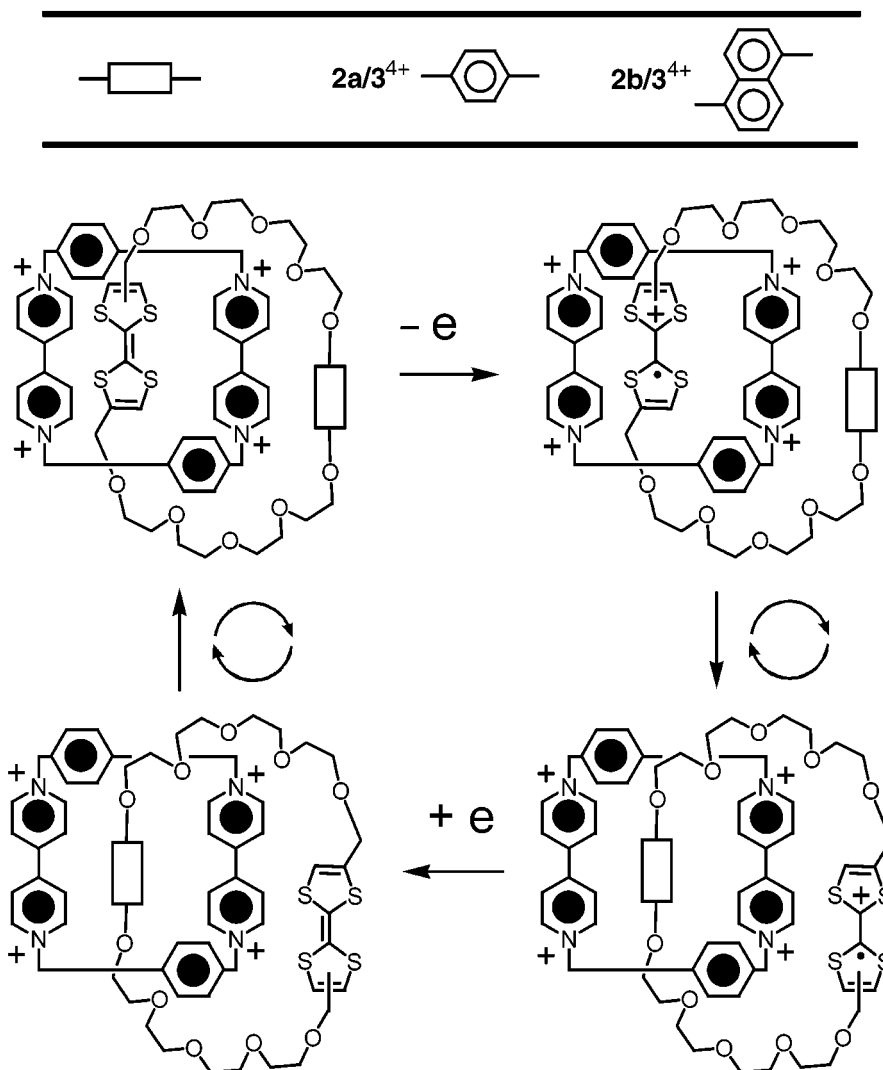


Figure 8. Schematic representation of the movements taking place in the [2]catenane **2a/3⁴⁺** upon oxidation/reduction of the TTF unit of its polyether component **2a**. Note that both redox-induced circumrotation movements can occur clockwise or anticlockwise with the same probability.

that oxidation is followed by a rearrangement taking place on the time scale of the electrochemical experiment.²³ The nature of this rearrangement has been elucidated by the following observations: (i) the second oxidation of the TTF unit is reversible, which shows that the system does not undergo any further rearrangement after one-electron oxidation, and (ii) the strongly positive potential value for the oxidation of the 1,4-dioxybenzene ring indicates that, when this process occurs, the 1,4-dioxybenzene ring is trapped within the tetracationic cyclophane.^{14,21} A very similar behavior is shown by the catenane **2b/3⁴⁺**.^{5e} These features show that, after the first oxidation of the TTF unit, the macrocyclic polyether circumrotates (Figure 8) with respect to the tetracationic cyclophane delivering the 1,4-dioxybenzene ring (catenane **2a/3⁴⁺**) or the 1,5-dioxynaphthalene ring system (catenane **2b/3⁴⁺**) into its cavity. Upon reduction of the cyclophane component of **2a/3⁴⁺** and **2b/3⁴⁺**, the well-known^{11,14} splitting of the first two-electron wave and the displacement of all the processes to more negative potentials are observed (**2a/3⁴⁺**: -0.32 V, -0.45 V, -0.86 V vs SCE, curve c in Figure 7; **2b/3⁴⁺**: -0.33 V, -0.49 V, -0.87 V vs SCE). It is interesting to note that the second monoelectronic reduction process, which involves the

"inside" bipyridinium unit, occurs in **2b/3⁴⁺** at a potential value 40 mV more negative than in **2a/3⁴⁺**. This difference can be explained by considering that the "inside" bipyridinium unit interacts with both donor groups of the crown ether, and that the dioxyaromatic unit contained in **2b**, namely the 1,5-dioxynaphthalene ring system, is a better donor than the 1,4-dioxybenzene ring incorporated in **2a**.

Pseudorotaxane 1a·3⁴⁺. Upon oxidation, the electroactive component of the pseudorotaxane **1a·3⁴⁺** is the acyclic polyether **1a**. In analogy with what was observed previously^{5d} for **1b·3⁴⁺**, the first anodic wave depends on the scan rate: at 200 mV s⁻¹, it merges (curve g in Figure 7) into the second oxidation wave, whose potential value is not scan-rate dependent and is also identical to that of free **1a**. These results are consistent with (i) the inclusion of the TTF unit inside the tetracationic cyclophane **3⁴⁺**, (ii) the displacement of **3⁴⁺** away from the TTF⁺ radical cation and (iii) the lack of any interaction

(23) The alternative explanation, based on lack of reversibility of the electrode process on account of restricted access to the "inside" TTF unit, can be ruled out on the basis of the behavior observed for all other catenanes and rotaxanes previously investigated. See, for example, refs 10 and 16a.

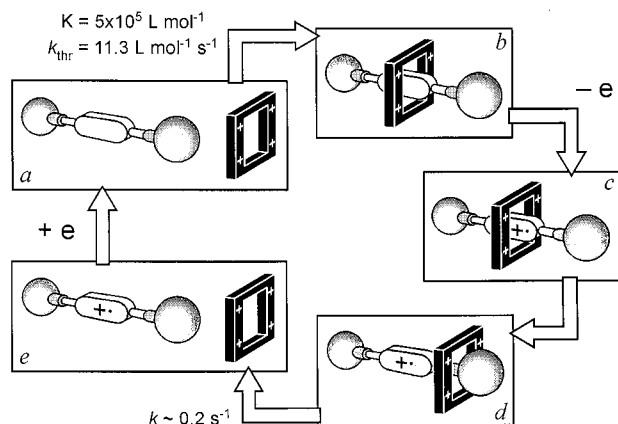


Figure 9. Schematic representation of the processes involving the [2]pseudorotaxane $1a \cdot 3^{4+}$ and its components in MeCN at room temperature upon oxidation/reduction of the TTF unit contained in dumbbell-shaped compound $1a$. The molecular components (a) self-assemble very efficiently, but slowly, to give the [2]pseudorotaxane $1a \cdot 3^{4+}$ (b). When the TTF unit contained in $1a$ is oxidized (c), the 3^{4+} ring moves far from it (d). At this point, the ring slowly slips over one of the bulky end groups, leading to dissociation of the [2]pseudorotaxane (e). Reduction of the TTF^+ radical cation back to the neutral state affords the initial situation (a).

between 3^{4+} and the oxidized forms of the TTF unit of the acyclic polyether.

The cathodic part of the scan of $1a \cdot 3^{4+}$ is complicated, in comparison with that of $1b \cdot 3^{4+}$, by the presence of the bulky *tert*-butylphenoxy end groups, which slow the dethreading and rethreading processes (vide supra). In the cyclic voltammetric pattern (curve g in Figure 7), the cathodic waves at +0.67 and +0.31 V correspond to the one-electron reduction of the TTF^{2+} dication and the TTF^+ radical cation, respectively, in the dethreaded acyclic polyether. The strongly scan-rate-dependent wave at +0.45 V is assigned to the reduction of the TTF^+ radical cation in the fraction of acyclic polyether still threaded through, but located far from, 3^{4+} . The scan-rate dependence of such a wave can be explained by considering that the repositioning of 3^{4+} on the restored TTF unit occurs on the time scale of the electrochemical experiment. This rather complex electrochemical behavior, along with the kinetic characterization of the threading and dethreading processes, is summarized graphically in Figure 9.

The reduction behavior of tetracationic cyclophane 3^{4+} in the pseudorotaxane $1a \cdot 3^{4+}$ is characterized by two important features (curve h in Figure 7): (i) the bipyridinium units undergo the first one-electron reduction at two different potential values, both negatively shifted in comparison to the free cyclophane, whereas they are reoxidized simultaneously at a potential which approaches that of the free cyclophane by increasing scan rate, and (ii) the simultaneous second one-electron reduction of the two units occurs reversibly at the same potential of the free cyclophane. These results indicate clearly that the one-electron reduction of the two bipyridinium units of $1a \cdot 3^{4+}$ causes the displacement of the reduced cyclophane far from the TTF unit of $1a$. The result described in point (i) is, at first sight, surprising since the first reduction process of the two bipyridinium units of $1a \cdot 3^{4+}$ is expected to occur at the same potential for a pseudorotaxane superstructure like that illustrated Figure 1. In fact, this is the case for several other

pseudorotaxanes and rotaxanes based on the 3^{4+} cyclophane.^{4b,5d,g,11} A splitting originating from electronic interactions between the two units²⁴ can be excluded because it is not observed for $1b \cdot 3^{4+}$. The assignment of the splitting to the dethreading/rethreading kinetics does not seem plausible, because the morphology of the cathodic part of the wave does not change on changing scan rate. Other possible explanations can be related to the presence of (i) two distinct pseudo-*cis*-rotaxane species, deriving from the *cis*- and *trans*-isomers associated with the TTF unit, (ii) two different coconformations, in very slow equilibrium, resulting from the way in which the polyether chains interact with the tetracationic cyclophane, or (iii) only one coconformation, where the two bipyridinium units of the cyclophane are not equivalent, as in the case of a "pseudocatenane" superstructure. The nearly 1:1 intensity ratio (curve h in Figure 7) of the two voltammetric waves can be explained straightforwardly by the third hypothesis, whereas hypotheses (i) and (ii) can hold only if the two species are present in equal amounts. It should also be noted that in the case of $1a \cdot 3^{4+}$, the presence of electron-donor units at the ends of the dumbbell-shaped component can account for formation of a "pseudocatenane" superstructure [hypothesis (iii)], and that the lack of splitting in $1b \cdot 3^{4+}$ disfavors hypotheses (i) and (ii).

The slowness of the (re)threading process is clearly evidenced by the following observations: (a) when the cathodic part of an oxidation scan is extended to negative potentials, the reduction behavior tends to that of free 3^{4+} ; (b) when the anodic part of a reduction scan is extended to positive potentials, the oxidation behavior tends to that of free $1a$; (c) after repeated oxidation (reduction) scans without renewing the diffusion layer, the voltammetric pattern of free $1a$ (free 3^{4+}) is observed.

From the above discussion, it is evident that the redox behavior of pseudorotaxane $1a \cdot 3^{4+}$ is very complicated. This situation is a consequence of the rotaxane-like character of this system.¹⁵ In this regard, comparison of the electrochemical properties of the pseudorotaxanes $1a \cdot 3^{4+}$ and $1b \cdot 3^{4+}$ with those of a "true" rotaxane, like, for example, $1c \cdot 3^{4+}$ (Figure 1), would be very interesting. Such an investigation is underway in our laboratories.

¹H NMR Spectroscopy. The ¹H NMR spectrum of a yellow CD₃CN solution of TTF shows a singlet centered on δ 6.43. After the addition of 2 equiv of *o*-chloroanil, the solution becomes brown and the singlet resonates at δ 6.32, suggesting the formation of an adduct.^{25,26} Upon addition of Na₂S₂O₅ and D₂O, the singlet resonance returns to δ 6.43 as the *o*-chloroanil is reduced and the adduct dissociates. When the same experiment is carried out in the presence of 3^{4+} , i.e., a tetracationic cyclophane which binds⁵ TTF inside its cavity, the singlet, observed at δ 6.17 for the protons of the TTF unit encircled by the cyclophane, shifts to δ 6.32 after the addition of *o*-chloroanil. Commensurate with this change in the spectrum, the resonance at δ 7.88 for the β -bipyridinium protons of the complexed 3^{4+} disappears and that associ-

(24) Kaifer and co-workers have found that the first reduction process of the two bipyridinium units of a rotaxane composed of 3^{4+} and a phenylenediamine-based dumbbell takes place at different potentials. They rationalized this result to "communication" of the two units through the interposed electron donor moiety, see: Córdova, E.; Bissell, R. A.; Kaifer, A. E. *J. Org. Chem.* **1995**, *60*, 1033–1038.

(25) For a report on an adduct formed between TTF and *p*-chloroanil, see: Mayerle, J. J.; Crowley, J. I. *Acta Crystallogr.* **1979**, *B35*, 2988–2995.

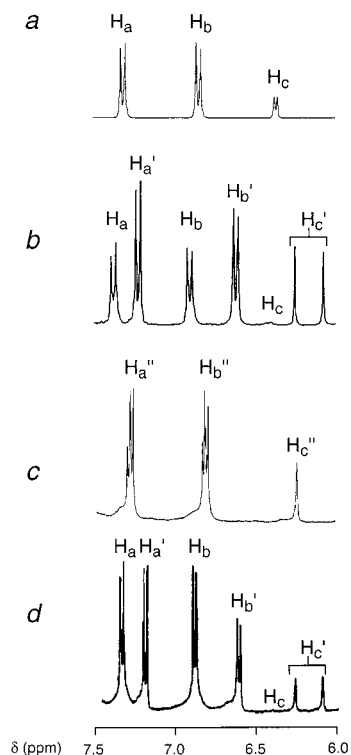


Figure 10. Partial ¹H NMR spectra (CD₃CN, 25 °C) (a) of the acyclic polyether **1a** and of an equimolar mixture of **1a** and **3**⁴⁺ (b) before and (c) after the addition of *o*-chloroanil, as well as (d) of the mixture of **1a**, **3**⁴⁺, and *o*-chloroanil after the addition of Na₂S₂O₅ and H₂O, followed by counterion exchange. The proton labels illustrated in (a), (b), and (d) are defined in Scheme 2. The phenylene and TTF protons of the adduct formed between **1a** and *o*-chloroanil are labeled H_a', H_b', and H_c'.

ated with the uncomplexed **3**⁴⁺ appears at δ 8.16. After the addition of Na₂S₂O₅ and H₂O, followed by counterion exchange,²⁷ the *o*-chloroanil is reduced and the original resonances of the complex between TTF and **3**⁴⁺ are again observed.

In the ¹H NMR spectrum of a CD₃CN solution of a mixture of the *cis*- and the *trans*-isomers of **1a**, the phenylene protons H_a and H_b give rise (Figure 10a) to an AA'BB' system. The TTF protons H_c appear as two equally intense singlets, indicating (i) that equimolar amounts of the *cis*- and *trans*-isomers are present in solution and (ii) that the isomerization is slow on the ¹H

(26) In a preliminary communication (see ref 5e) we reported that the TTF-containing [2]catenane **2b/3**⁴⁺ undergoes a conformational change upon addition of *o*-chloroanil. It was believed that the TTF unit, originally located inside the cavity of the tetracationic cyclophane component, was oxidized to its dicationic form upon addition of *o*-chloroanil. Electrostatic repulsion between the newly formed TTF²⁺ dication and the tetracationic cyclophane component was invoked as being responsible for the observed conformational change. However, subsequent and more rigorous ¹H NMR spectroscopic experiments have shown that TTF is *not* oxidized by *o*-chloroanil. In particular, the ¹H NMR spectrum of a CD₃CN solution of TTF and *o*-chloroanil does *not* show paramagnetic peak broadening suggesting that the radical cation TTF^{•+} is not formed. Also, the characteristic resonance associated with the protons of the TTF²⁺ dication (ca. δ 9.5) are *not* observed. Instead, the ¹H NMR spectrum exhibits a sharp singlet (δ = 6.32) in the region where the protons of neutral TTF are expected to resonate. Most likely, the conformational change associated with the [2]catenane **2b/3**⁴⁺ results from an adduct formation between the TTF unit and *o*-chloroanil.

(27) After the addition of Na₂S₂O₅ and H₂O, an excess of NH₄PF₆ was added. The solvent was removed under reduced pressure, and the residue was washed with H₂O. The resulting green solid was dissolved in CD₃CN and analyzed by ¹H NMR spectroscopy.

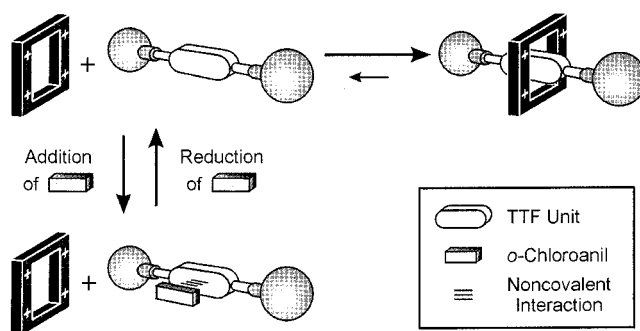


Figure 11. Diagrammatic representation of the chemically controlled switching of the [2]pseudorotaxane **1a·3**⁴⁺.

NMR time scale at 25 °C. Upon mixing equimolar amounts of **1a** and **3**[PF₆]₄ in CD₃CN, a green color develops, indicating the formation (Scheme 2) of the 1:1 complex **1a·3**⁴⁺. In the ¹H NMR spectrum of this solution, distinct signals for both the complexed and uncomplexed species are observed, demonstrating that the complexation/decomplexation process is slow on the ¹H NMR time scale at 25 °C. Two AA'BB' systems are observed (Figure 10b) for the phenylene protons of the complexed (H_a' and H_b') and uncomplexed (H_a and H_b) species. After the addition of *o*-chloroanil, extrusion of the TTF unit from the cavity of **3**⁴⁺ occurs presumably as a result of the formation of an adduct between **1a** and *o*-chloroanil. Consequently, the signals associated with **1a·3**⁴⁺ are not present²⁸ (Figure 10c) in the corresponding ¹H NMR spectrum. Upon addition of Na₂S₂O₅ and H₂O, followed by counterion exchange,²⁷ *o*-chloroanil is reduced and the complex **1a·3**⁴⁺ reforms (compare Figures 10b and 10d). The overall process involving the chemically controlled²⁹ switching of the [2]pseudorotaxane **1a·3**⁴⁺ is summarized in Figure 11. An equilibrium between the complexed and uncomplexed species exists in solution, favoring the former. However, the addition of *o*-chloroanil is accompanied by the formation of an adduct with the guest, thus perturbing the equilibrium as a result of the [2]pseudorotaxane dissociating. After the reduction of *o*-chloroanil, the guest is released and the original equilibrium between the [2]pseudorotaxane and its separate components is restored.

The ¹H NMR spectra of CD₃CN solutions of the macrocyclic polyethers **2a** and **2b** show (Figures 12a and 13a) one set of signals for the 1,4-dioxybenzene protons H_{db} and for the 1,5-dioxynaphthalene protons H-2/6, respectively. In both instances, two equally intense singlets are observed for the TTF protons H_{ttf} as a result of the presence of *cis*- and *trans*-isomers in solution. In the [2]catenanes **2a/3**⁴⁺ and **2b/3**⁴⁺, one of the two isomers is stabilized (probably the *trans*-isomer, Figure 2) relative to the other and the TTF protons give rise

(28) Only the signals of the free tetracationic cyclophane **3**⁴⁺ and those of the adduct formed between **1a** and *o*-chloroanil are observed. Interestingly, the resonances associated with the protons H_a', H_b', and H_c' of the adduct resonate (Figures 10a and 10c) at fields higher than those associated with the protons H_a, H_b, and H_c of free **1a**. In addition, while the protons H_a and H_b give rise to an AA'BB' system, a complex pattern is observed for the protons H_a' and H_b'.

(29) For examples of the reversible chemically controlled switching of [2]pseudorotaxanes as a result of the competitive formation of adducts, see: (a) Ballardini, R.; Balzani, V.; Credi, A.; Gandolfi, M. T.; Langford, S. J.; Menzer, S.; Prodi, L.; Stoddart, J. F.; Venturi, M.; Williams, D. J. *Angew. Chem., Int. Ed. Engl.* **1996**, *35*, 978–981. (b) Credi, A.; Balzani, V.; Langford, S. J.; Stoddart, J. F. *J. Am. Chem. Soc.* **1997**, *119*, 2679–2681.

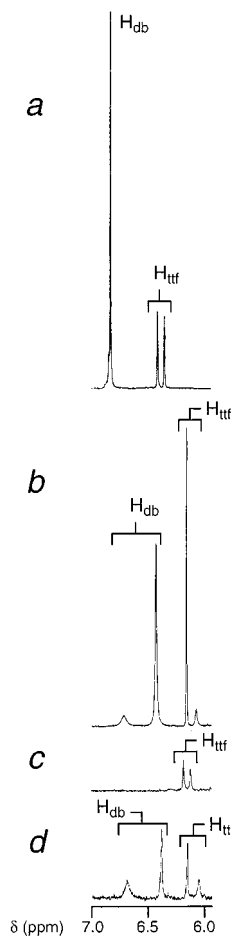


Figure 12. Partial ¹H NMR spectra (CD₃CN, 25 °C) (a) of the macrocyclic polyether **5a** and of the [2]catenane **2a/3**⁴⁺ (b) before and (c) after the addition of *o*-chloroanil, as well as (d) of the mixture of **2a/3**⁴⁺ and *o*-chloroanil after the addition of Na₂S₂O₅ and H₂O, followed by counterion exchange. The proton labels are defined in Scheme 1.

(Figures 12b and 13b) to two singlets of different intensities. Similarly, the 1,4-dioxybenzene protons in **2a/3**⁴⁺ and the 1,5-dioxynaphthalene protons in **2b/3**⁴⁺ resonate as two sets of signals of different intensities. However, the characteristic upfield resonances, which are normally observed^{30,31} for the protons of dioxyarene rings sandwiched between two bipyridinium units, are not detected in either case. These observations suggest that the dioxyarene rings are located alongside the cavity of tetracationic cyclophane component and that the TTF units are positioned inside³² in both these [2]catenanes. Addition of *o*-chloroanil to the CD₃CN solutions of **2a/3**⁴⁺ and **2b/3**⁴⁺ exchanges the “inside” and “alongside” units, presumably, as a result of the formation of adducts between their TTF units and *o*-chloroanil. The corresponding ¹H NMR spectra show (Figures 12c and 13c) a

(30) The protons H_{db} of a 1,4-dioxybenzene ring located inside the cavity of **3**⁴⁺ resonate (see ref 14) in the region of δ = 3.0–3.5.

(31) The protons H-4/8 of a 1,5-dioxynaphthalene ring system located inside the cavity of **3**⁴⁺ resonate in the region of δ = 2.1–2.6. For examples, see: Asakawa, M.; Ashton, P. R.; Boyd, S. E.; Brown, C. L.; Gillard, R. E.; Kocian, O.; Raymo, F. M.; Stoddart, J. F.; Tolley, M. S.; White, A. J. P.; Williams, D. J. *J. Org. Chem.* **1997**, 62, 26–37.

(32) The location of the TTF unit inside the cavity of the tetracationic cyclophane was confirmed by the cross-peaks between the protons of the methylene groups attached to this unit and both the α-bipyridinium and the *p*-phenylene protons observed in a 2D ROESY spectrum.

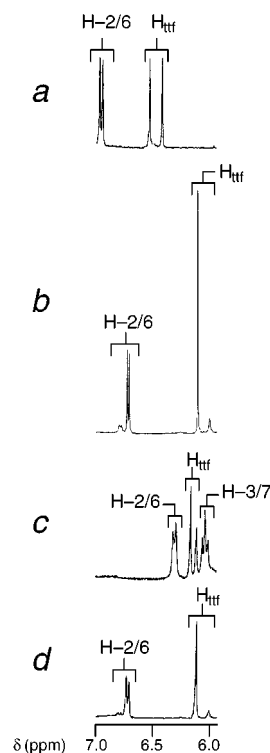


Figure 13. Partial ¹H NMR spectra (CD₃CN, 25 °C) (a) of the macrocyclic polyether **5** and of the [2]catenane **2b/3**⁴⁺ (b) before and (c) after the addition of *o*-chloroanil, as well as (d) of the mixture of **2b/3**⁴⁺ and *o*-chloroanil after the addition of Na₂S₂O₅ and H₂O, followed by counterion exchange. The proton labels are defined in Scheme 2.

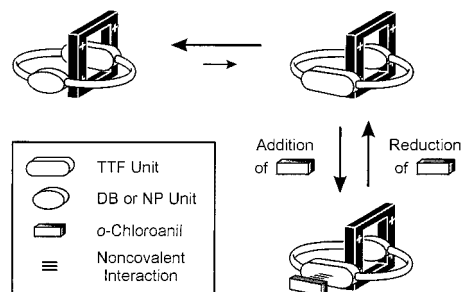


Figure 14. Diagrammatic representation of the chemically controlled switching of the [2]catenanes **2a/3**⁴⁺ and **2b/3**⁴⁺. DB and NP stand for the 1,4-dioxybenzene and 1,5-dioxynaphthalene unit, respectively.

change in the chemical shift and relative intensities of the two singlets associated with the TTF protons. In addition, dramatic upfield shifts of the resonances associated with the 1,4-dioxybenzene protons H_{db} (Δδ ca. –3 ppm) and with the 1,5-dioxynaphthalene protons (Δδ ca. –5 ppm) demonstrate that these units are now encircled by the cyclophane component. Reduction of *o*-chloroanil destroys its ability to form adducts with the TTF units of the [2]catenanes which reinsert themselves back into the cavities. After the addition of Na₂S₂O₅ and H₂O to both solutions and counterion exchange,²⁷ the original resonances for the dioxyarene and TTF protons are observed (compare Figures 12b and 12d as well as Figures 13b and 13d). The overall process, involving the chemically controlled²⁹ switching of the [2]catenanes **2a/3**⁴⁺ and **2b/3**⁴⁺, is summarized in Figure 14.

Conclusions

We have synthesized the TTF-containing polyether **1a** which associates ($K_{\text{ass}} = 5 \times 10^5 \text{ L mol}^{-1}$ at 296 K in MeCN) under thermodynamic control with the tetracationic cyclophane **3**⁴⁺ in solution to form the [2]pseudorotaxane **1a**·**3**⁴⁺. We have prepared the TTF-containing macrocyclic polyethers **2a** and **2b** in yields of 49 and 55%, respectively. These macrocyclic polyethers have been used as templates in the kinetically controlled self-assembly of [2]catenanes **2a/3**[PF₆]₄ and **2b/3**[PF₆]₄ which were isolated in yields of 43 and 23%, respectively. The spectroscopic investigations of these compounds have shown that, while TTF²⁺ exhibits a strong fluorescence, no emission can be observed for the TTF²⁺ units contained in the polyethers and in the corresponding pseudorotaxanes and catenanes. The results obtained in the electrochemical experiments and upon addition of Fe(ClO₄)₃ or *o*-chloranil show clearly that oxidation or adduct formation of the TTF unit of the polyethers in **1a**·**3**⁴⁺ and in **2a/3**⁴⁺ and **2b/3**⁴⁺ and reduction of the cyclophane in **1a**·**3**⁴⁺ cause extensive mechanical movements. More specifically, such rearrangements involve the circumrotation of one ring with respect to the other in **2a/3**⁴⁺ and in **2b/3**⁴⁺ (Figure 9), and the displacement of the ring along the thread, ultimately leading to dethreading, in **1a**·**3**⁴⁺ (Figure 10). In all cases, the movements can be fully reversed by electrochemical or chemical inputs.

Experimental Section

General Methods. Solvents were purified according to literature procedures.³³ The compounds **1b**,^{5d} **4**,⁸ **5a**,¹⁴ **6**[PF₆]₂,¹⁴ **5b**,³⁴ and **3**[PF₆]₄³⁵ were synthesized according to literature procedures. Thin-layer chromatography (TLC) was carried out using aluminum sheets, precoated with silica gel 60F or aluminum oxide 60F₂₅₄ neutral. The plates were inspected by UV-light prior to development with iodine vapor or by treatment with ceric ammonium molybdate reagent and subsequent heating. Melting points are uncorrected. ¹H NMR and ¹³C NMR spectra were recorded on a 300 and a 75 MHz spectrometer, respectively. The equipment and procedures used for absorption, luminescence, and electrochemical measurements have been previously reported.¹⁰ For the electrochemical experiments it is worth noting that the concentration of the electroactive species was of the order of 10⁻⁴ mol L⁻¹ and that 0.05 mol L⁻¹ tetraethylammonium hexafluorophosphate was added as supporting electrolyte. Ru(bpy)₃²⁺ [*E*_{1/2}(Ru³⁺/Ru²⁺) = +1.290 V and *E*_{1/2}(Ru²⁺/Ru⁺) = -1.330 V vs SCE]³⁶ was present in the solution as an internal reference. Cyclic voltammograms (CV) were obtained at sweep rates of 10, 20, 50, 100, 200, 500, and 1000 mV s⁻¹; differential pulse voltammograms (DPV) were performed with a scan rate of 20 mV s⁻¹, a pulse height of 75 mV, and a duration of 40 ms. For reversible processes the same halfwave potential values were obtained from the DPV peaks and from an average of the cathodic and anodic cyclic voltammetric peaks. The potential values for not fully reversible processes were estimated from the DPV peaks. The experimental error on the potential values for reversible and not fully reversible processes was estimated to be ±5 and ±10 mV, respectively.

(33) Perrin, D. D.; Armarego, W. L. *Purification of Laboratory Chemicals*, 3rd ed.; Pergamon Press: New York, 1988.

(34) Ashton, P. R.; Huff, J.; Parsons, I. W.; Preece, J. A.; Stoddart, J. F.; Williams, D. J.; White, A. J. P.; Tolley, M. S. *Chem. Eur. J.* **1996**, *2*, 123–136.

(35) Asakawa, M.; Dehaen, W.; L'abbé, G.; Menzer, S.; Nouwen, J.; Raymo, F. M.; Stoddart, J. F.; Williams, D. J. *J. Org. Chem.* **1996**, *61*, 9591–9595.

(36) Juris, A.; Balzani, V.; Barigelli, F.; Campagna, S.; Belser, P.; von Zelewsky, A. *Coord. Chem. Rev.* **1988**, *84*, 85–277.

4,4'(5')-Bis[2-[2-[2-(4-*tert*-butylphenoxy)ethoxy]ethoxy]-ethoxymethylene]tetrathiafulvalene (1a**).** The diol **4** (110 mg, 0.4 mmol) was added to a suspension of NaH (48 mg, 2.0 mmol) in dry and degassed THF (30 mL), and the mixture was heated under reflux and an atmosphere of Ar for 1 h. A solution of the bistosylate **8** (436 mg, 1.0 mmol) in dry and degassed THF (20 mL) was added dropwise over 45 min. The mixture was heated under reflux for a further 24 h. After cooling to room temperature, wet THF was added and the solvent was removed under reduced pressure. The residue was suspended in CH₂Cl₂ and washed with a saturated aqueous solution of K₂CO₃ and H₂O, and dried (MgSO₄). The solvent was removed under reduced pressure, and the residue was purified by column chromatography (SiO₂, CH₂Cl₂/MeOH, 99:1) to afford **1a** (264 mg, 80%) as a yellow-orange oil. LSIMS: *m/z* = 792 [M]⁺; ¹H NMR (CD₃CN): δ = 7.32 (d, 4H), 6.83 (d, 4H), 6.34 (s, 1H), 6.32 (s, 1H), 4.23 (s, 4H), 4.08–4.00 (m, 4H), 3.78–3.70 (m, 4H), 3.63–3.47 (m, 16H), 1.27 (s, 18H); ¹³C NMR (CD₃CN): δ = 157.4, 144.1, 135.5, 127.1, 118.7, 117.6, 117.2, 114.7, 71.6, 71.2, 71.1, 70.9, 70.8, 70.2, 70.0, 68.4, 68.2, 34.5, 32.3, 31.6. Anal. Calcd for C₄₀H₅₆O₈S₄: C = 60.57, H = 7.12, S = 16.17. Found: C = 60.40, H = 6.96, S = 16.3.

[2]Pseudorotaxane 1a·3[PF₆]₄. Equimolar amounts (25 mM) of **1a** and **3**[PF₆]₄ were mixed in CD₃CN. The solvent was distilled off under reduced pressure to afford **1a·3**[PF₆]₄ as a green solid. ¹H NMR (CD₃CN): δ = 9.10–8.82 (m, 8H), 7.85–7.55 (m, 16H), 7.15 (d, 4H), 6.54 (d, 4H), 6.17 (s, 1H), 6.00 (s, 1H), 5.67 (s, 4H), 5.66 (s, 4H), 4.16 (s, 2H), 4.12 (s, 2H), 4.08–4.00 (m, 4H), 3.90–3.67 (m, 12H), 3.65–3.52 (m, 8H), 1.21 (s, 9H), 1.20 (s, 9H). Anal. Calcd for C₇₆H₈₈F₂₄N₄O₈P₄S₄: C = 48.20, H = 4.68, N = 2.96, S = 6.77, found: C = 48.20, H = 4.72, N = 2.72, S = 6.90.

Macrocyclic Polyether 2a. A solution of the diol **4** (264 mg, 1.0 mmol), the bistosylate **5a** (770 mg, 1.0 mmol), LiBr (40 mg, 0.5 mmol), and CsOTf (40 mg, 0.1 mmol) in dry and degassed THF (260 mL) was added dropwise over 20 h to a suspension of NaH (120 mg, 5.0 mmol) in dry and degassed THF (300 mL) heated under reflux and an atmosphere of Ar. The mixture was heated under reflux for a further 4 d. After being cooled to room temperature, the solvent was removed under reduced pressure. The residue was partitioned between CH₂Cl₂ and H₂O, and the aqueous layer was washed with CH₂Cl₂. The combined organic layers were washed with 10% aqueous NaOH (50 mL), 5% aqueous HCl, and 5% aqueous K₂CO₃, H₂O and dried (MgSO₄). The solvent was removed under reduced pressure, and the residue was purified by column chromatography (SiO₂, CH₂Cl₂/MeOH, 98:2) to afford **2a** (338 mg, 49%) as a yellow-orange oil. LSIMS: *m/z* = 690 [M]⁺; ¹H NMR (CD₃CN): δ = 6.82 (s, 4H), 6.39 (s, 1H), 6.32 (s, 1H), 4.24 (s, 4H), 4.05–3.95 (m, 4H), 3.77–3.70 (m, 4H), 3.65–3.50 (m, 24H); ¹³C NMR (CD₃CN): δ = 153.8, 135.4, 117.6, 116.2, 71.2, 71.1, 70.3, 70.1, 69.9, 68.8, 68.4, 68.3. Anal. Calcd for C₃₀H₄₂O₁₀S₄: C = 52.18, H = 6.13, S = 18.57. Found: C = 52.19, H = 6.32, S = 18.2.

Macrocyclic Polyether 2b. A solution of the diol **4** (925 mg, 3.5 mmol), the dibromide **5b** (2240 mg, 3.5 mmol), LiBr (40 mg, 0.5 mmol), and CsOTf (40 mg, 0.1 mmol) in dry and degassed THF (260 mL) was added dropwise over 20 h to a suspension of NaH (288 mg, 12.0 mmol) in dry and degassed THF (280 mL) heated under reflux and an atmosphere of Ar. The mixture was heated under reflux for a further 4 d. After being cooled to room temperature, the solvent was removed under reduced pressure. The residue was partitioned between CH₂Cl₂ and H₂O, and the aqueous layer was washed with CH₂Cl₂. The combined organic layers were washed with a saturated aqueous solution of NaCl and then with H₂O and finally dried (MgSO₄). The solvent was removed under reduced pressure, and the residue was subjected to column chromatography (SiO₂, CH₂Cl₂/MeOH, 30:1) to afford **2b** (1.61 g, 55%) as a yellow wax. LSIMS: *m/z* = 740 [M]⁺; ¹H NMR (CD₃CN): δ = 7.84–7.77 (m, 2H), 7.41–7.31 (m, 2H), 6.95–6.85 (m, 2H), 6.52 (s, 1H), 6.42 (s, 1H), 4.28–4.18 (m, 4H), 3.94–3.84 (m, 6H), 3.72–3.40 (m, 26H); ¹³C NMR (CD₃CN): δ = 155.3, 127.6, 126.5, 118.6, 115.1, 106.9, 73.4, 72.1, 71.6, 71.2, 70.4, 70.2, 69.1,

62.0, 51.9. Anal. Calcd for $C_{34}H_{44}O_{10}S_4$: C = 55.11, H = 5.99, S = 17.31. Found: C = 54.99, H = 5.98, S = 17.4.

[2]Catenane 2a/3[PF₆]₄. A solution of **2a** (200 mg, 0.3 mmol), **6**[PF₆]₂ (353 mg, 0.5 mmol), and **7** (132 mg, 0.5 mmol) in dry and degassed DMF (15 mL) was stirred for 6 d at ambient temperature. The solvent was removed under reduced pressure, and the residue was purified by column chromatography (SiO₂, MeOH/2 M NH₄Cl_{aq}/MeNO₂, 7:2:1.7). The resulting green solid was dissolved in H₂O. After the addition of a saturated aqueous solution of NH₄PF₆, **2a/3**[PF₆]₄ precipitated out of solution and was isolated (223 mg, 43%) as a green solid. Mp > 250 °C; LSIMS: m/z = 1790 [M]⁺, 1645 [M - PF₆]⁺, 1500 [M - 2PF₆]⁺, 1355 [M - 3PF₆]⁺; ¹H NMR (CD₃CN): δ = 9.07–8.80 (m, 8H), 7.90–7.60 (m, 16H), 6.72–6.37 (s, 4H), 6.15–6.03 (s, 2H), 5.60–5.80 (m, 8H), 4.30–4.13 (m, 4H), 3.95–3.45 (m, 32H); ¹³C NMR (CD₃CN): δ = 153.4, 145.7, 145.2, 144.6, 136.8, 134.0, 131.7, 128.4, 126.4, 126.1, 119.6, 116.1, 108.6, 71.9, 71.6, 71.3, 70.8, 70.6, 70.5, 70.1, 68.7, 68.5, 65.4. Anal. Calcd for $C_{66}H_{74}F_{24}N_4O_{10}P_4S_4$: C = 44.25, H = 4.16, N = 3.13, S = 7.16. Found: C = 43.95, H = 4.18, N = 3.03, S = 7.30.

[2]Catenane 2b/3[PF₆]₄. A solution of **2b** (1390 mg, 1.9 mmol), **6**[PF₆]₂ (1330 mg, 1.9 mmol), and **7** (496 mg, 1.9 mmol) in dry and degassed DMF (125 mL) was stirred for 6 d at ambient temperature. The solvent was removed under reduced pressure and the residue was purified by column chromatography (SiO₂, MeOH/2 M NH₄Cl_{aq}/MeNO₂, 4:1.5:1.5). The resulting green solid was dissolved in H₂O. After the addition of a saturated aqueous solution of NH₄PF₆, **2b/3**[PF₆]₄ precipitated out of solution and was isolated (808 mg, 23%) as a

green solid. Mp > 300 °C; LSIMS: m/z = 1840 [M]⁺, 1695 [M - PF₆]⁺, 1551 [M - 2PF₆]⁺, 1406 [M - 3PF₆]⁺; ¹H NMR (CD₃CN): δ = 9.00–8.85 (m, 4H), 8.75–8.65 (m, 4H), 7.70–7.60 (m, 10H), 7.60–7.40 (m, 4H), 7.37–7.32 (m, 4H), 7.31–7.24 (m, 2H), 6.73–6.68 (m, 2H), 6.08 (br s, 2H), 5.78–5.55 (m, 8H), 4.08 (br s, 4H), 4.00–3.50 (m, 32H); ¹³C NMR (CD₃CN): δ = 154.6, 146.4, 145.5, 144.3, 143.9, 136.7, 133.5, 126.9, 125.3, 125.0, 119.8, 114.6, 106.6, 72.0, 71.6, 71.3, 71.1, 70.7, 70.5, 70.4, 68.6, 68.5, 65.2. Anal. Calcd for $C_{70}H_{76}F_{24}N_4O_{10}S_4P_4$: C = 45.66, H = 4.16, N = 3.04, S = 6.96. Found: C = 45.55, H = 4.28, N = 3.18, S = 7.1. Details of the X-ray structural determination have been already reported^{5e} and deposited with the Cambridge Crystallographic Data Centre as supplementary publication no. CCDC-100460. Copies of the data can be obtained free of charge on application to the Director, CCDC, 12 Union Road, Cambridge CB2 1EZ (Fax: Int. code + (1223) 336 033; e-mail: deposit@chemcryst.cam.ac.uk).

Acknowledgment. This research was supported by the Engineering and Physical Sciences Research Council in the United Kingdom and by the University of Bologna (Funds for Selected Research Topics) and MURST (Supramolecular Devices project) in Italy, and by the EU (TMR grant FMRX-CT96-0076). We thank A. M. Talarico for help with some electrochemical experiments and L. Ventura for technical assistance. We thank graduate student Anthony R. Pease at UCLA for his design of the front cover.

JO991781T